PRAMANA
— journal of
physics

Vol. 63, No. 2
August 2004
pp. 321–326

Carbide precipitates in solution-quenched PH13-8 Mo stainless steel: A small-angle neutron scattering investigation

D SEN[1], A K PATRA[1], S MAZUMDER[1], J MITTRA[2], G K DEY[2] and P K DE[2]
[1]Solid State Physics Division; [2]Materials Science Division, Bhabha Atomic Research Centre, Mumbai 400 085, India
E-mail: debasis@apsara.barc.ernet.in

Abstract. This paper deals with the small-angle neutron scattering (SANS) investigation on solution-quenched PH13-8 Mo stainless steel. From the nature of the variation of the functionality of the profiles for varying specimen thickness and also from the transmission electron microscopy (TEM), it has been established that the small-angle scattering signal predominantly originates from the block-like metallic carbide precipitates in the specimen. The contribution due to double Bragg reflection is not significant in the present case. The single scattering profile has been extracted from the experimental profiles corresponding to different values of specimen thickness. In order to avoid complexity and non-uniqueness of the multi-parameter minimization for randomly oriented polydisperse block-like precipitate model, the data have been analyzed assuming randomly oriented polydisperse cylindrical particle model with a locked aspect ratio.

Keywords. Small-angle neutron scattering; carbide precipitates, steel.

PACS Nos 61.12.Ex

1. Introduction

Precipitation in alloy system is a subject of continuing scientific and technological interest [1,2]. PH 13-8 Mo steel is a precipitation-hardened steel, which is capable of achieving high strength and hardness with good corrosion resistance properties. Hence, the steel is used in aircraft, nuclear reactor, petrochemical plants and many other industries. However, presence of carbide formers such as Mo and Cr warrants the possibility of carbide precipitates in the structure and in turn affects the mechanical properties. Small-angle neutron scattering (SANS) is an important non-destructive technique to investigate the morphology and size distribution of such precipitates in mesoscopic length scale.

PH 13-8 Mo stainless steel (nominal composition in wt%: Cr 12.25–13.25, Ni 7.5–8.5, Mo 2–2.5, Al 0.9–1.35, C $0.5_{\max}$, P $0.01_{\max}$, Si $0.1_{\max}$, S $0.008_{\max}$, Fe balance) is a martensitic grade steel.

In the present investigation, small-angle neutron scattering (SANS) measurements have been used to investigate the structure of the carbide precipitates.

2. Experimental

Wrought PH 13-8 Mo steel sample of $10 \times 10 \times 10$ mm^3 size has been solution-quenched from 1000°C to ice floating water (specimen 1). The surfaces of the sample were ground significantly to remove the effect of oxidation on the outer layer. Figure 1 shows typical microstructure of metallic carbide precipitates. Thinner sample of size $10 \times 10 \times 2$ (thick) mm^3 (specimen 2) was sliced from the specimen 1 with a slow diamond saw. SANS experiments have been performed using a double crystal based small-angle neutron scattering instrument at the Guide Tube Laboratory of Dhruva reactor at Trombay, India [3]. The scattered intensities have been recorded as a function of wave vector transfer $q(= 4\pi \sin(\theta)/\lambda$, where 2θ is the scattering angle and $\lambda(= 0.312$ nm) is the incident neutron wavelength for the present experiment). SANS experiments have been performed for three perpendicular orientations of a specimen of thickness 1.0 cm. Since the sample is a strong scatterer, SANS measurements have been carried out for two different values of thickness, namely, 1.0 and 0.2 cm (specimens 1 and 2), respectively. Figure 2 depicts the background, transmission and resolution corrected SANS profiles in absolute scale for specimen 2 and also for the three perpendicular orientations

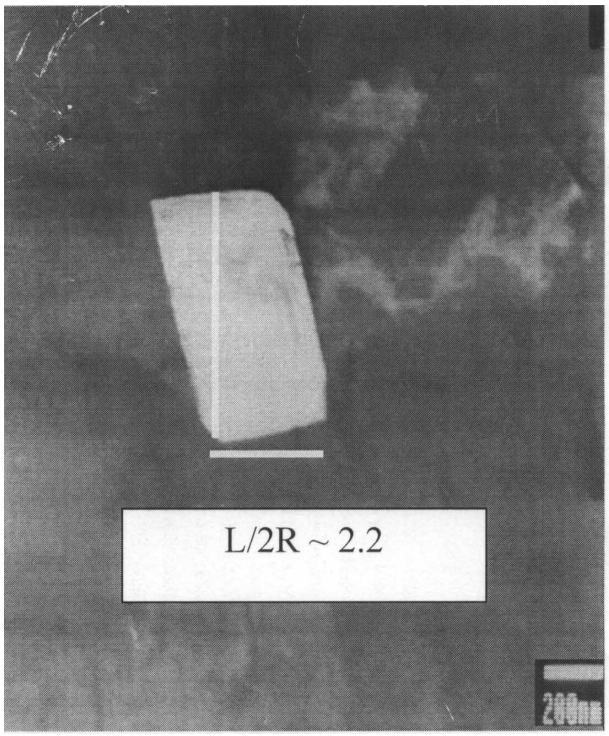

Figure 1. Dark field TEM micrograph of the block-like metallic precipitates. Selected area electron diffraction confirms that these as Mo- and Cr-based carbide precipitates.

of specimen 1. The inset shows the comparison of the functionality of the profiles by normalizing the profiles at the lowest available q value.

3. Data analysis and results

It is evident from figure 2 that the SANS profiles, from the three perpendicular orientations of specimen 1, resemble each other. This indicates that the system is isotropic as far as scattering is concerned. It is observed that the SAS signal falls as $q^{-4.3}$ at higher q region. For a polycrystalline sample like PH13-8 Mo stainless steel, the so-called scattering signal around direct beam may originate due to the true small-angle scattering from the randomly oriented particles and/or from double Bragg reflections (DBR) from the identical but slightly mis-oriented crystal planes. As the specimen is a polycrystalline one, the occurrence of scattering at small angle because of DBR remains a possibility. It is worth mentioning that the scattering signal from the *inter-grain* DBR varies as q^{-1} and is expected to diverge at very small q region [4]. But from the nature of the observed scattering profiles as depicted in figure 2, it is clear that the *inter-grain* DBR contribution is insignificant.

For scattering signal arising from inter-grain DBR, the functionality of the scattering profile remains unchanged although the scale factor changes with variation of specimen thickness. From figure 2, it is evident that the profile from specimen 2 is significantly sharper than that of specimen 1. Hence, it is concluded that the SANS signal in the present case is not arising from intra-grain DBR also.

The broadening of the profile with increasing specimen thickness can only be explained if the scattering profile is attributed to the multiple small-angle scattering [5,6] from the inhomogeneities in the system. From the scattering profiles of the specimens of two different thickness values, the single scattering profile has been estimated (inset figure 2) [7,8].

The dark field-TEM micrograph (figure 1) shows that the typical shape of the metallic carbide precipitate is block-like. Here it should be mentioned that TEM also indicated (not shown here) the presence of some needle-shaped retained austenites in the specimen. However, the neutron scattering contrast between the austenites and the matrix is very much weak compared to that between the carbide precipitates and the matrix and hence the SANS signal is attributed predominantly due to the carbide precipitates. TEM micrograph in figure 1 indicates that polydisperse spherical particle model cannot be considered for the analysis of the SANS data in the present situation. It is noteworthy that in practice it is very complicated to obtain, from experimental SANS data, the size distributions for an ensemble of randomly oriented block-like precipitates, with polydispersity in three perpendicular directions. Further, in such a situation one has to numerically minimize several non-linear parameters while fitting the model to the data and the question regarding the uniqueness of the estimated parameters remains unreciprocated.

Even in the case of cylindrical particles it is complicated enough in practice to carry out the analysis if the polydispersity in both radius R and length L are

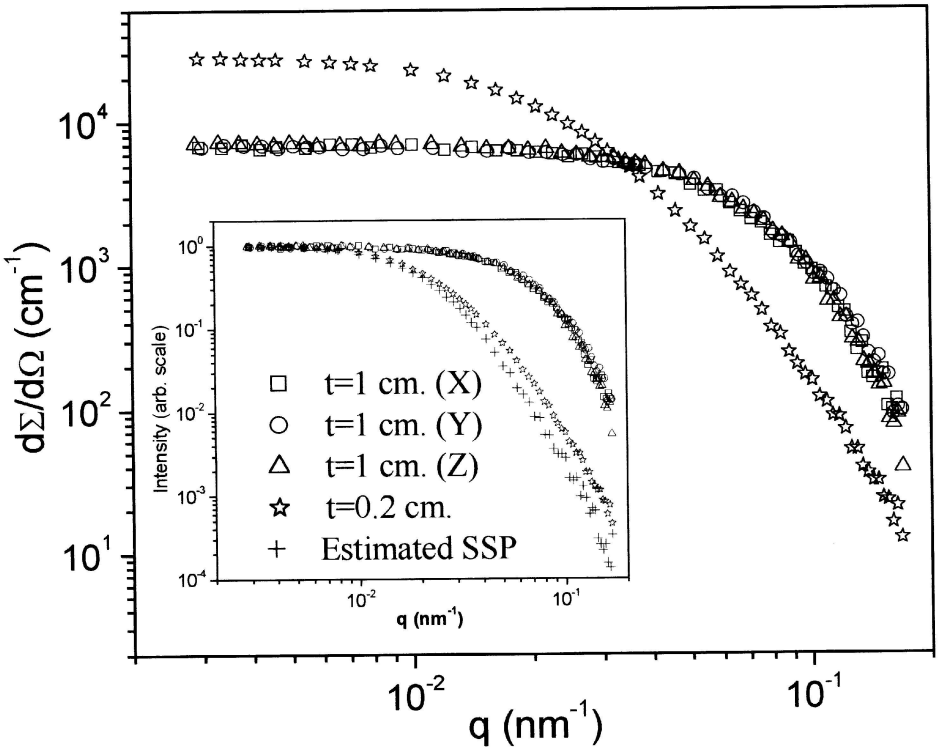

Figure 2. Transmission background and resolution corrected SANS data from PH 13-8 Mo. Estimated single scattering profile in the inset is compared with the profiles for two different values of specimen thickness.

considered separately for the precipitates. However, fortunately the situation can be handled if it is assumed that a locked aspect ratio ($\beta = L/(2R)$) of length to diameter exists for the cylinders [9] and an exponential/power law unified approach [10] is used for the structure factor. The parameters describing the radius distribution (log-normal) and the aspect ratio β were kept as fitting parameters while fitting the model to the single scattering profile. Length distribution was estimated from the estimated aspect ratio and the radius distribution. Estimated length distribution is depicted in figure 3. The important parameters of the estimated distributions are tabulated in table 1. The fit of the model to the estimated single scattering profile is shown in figure 4. It is seen that the average aspect ratio (3.4) estimated from SANS is somewhat more than that shown in the dark field TEM (2.2) in figure 1. This is because of the fact that the information obtained from SANS is statistically averaged information over a large number of precipitates, which is not the case for TEM. Further the possibility of different aspect ratio for the different precipitates as well as polydispersity in precipitates' shape cannot be ruled out in such a multi-component alloy.

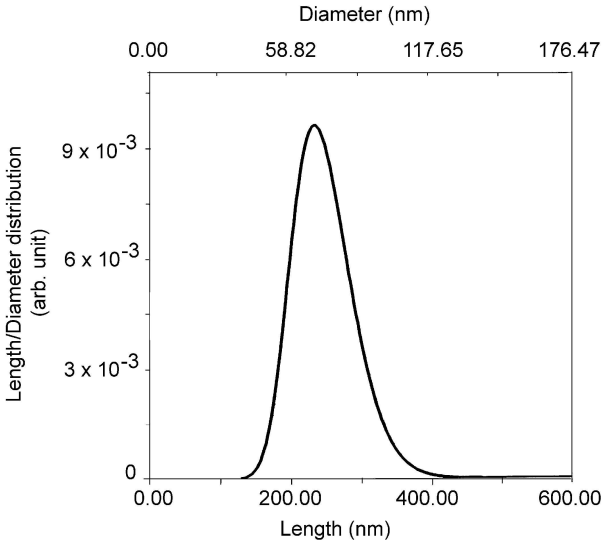

Figure 3. Length and diameter distribution of the precipitates estimated from SANS analysis for a cylindrical particle model with locked aspect ratio (described in the text).

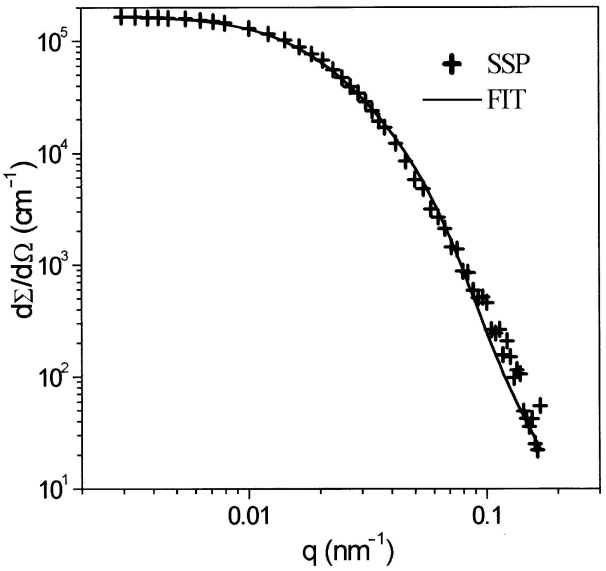

Figure 4. The fit of the polydisperse cylindrical particle model with locked aspect ratio (described in the text) to the estimated single scattering profile.

4. Conclusions

Strong small-angle neutron scattering signal from solution-quenched PH13-8 Mo stainless steel originates predominantly from undissolved block-like metallic carbide

Table 1. Important parameters of the estimated distributions ($\langle\ \rangle$ indicates average value).

$\langle L \rangle$ (nm)	$(\langle L \rangle^2 - \langle L \rangle^2)^{1/2}$ (nm)	$\langle R \rangle$ (nm)	$(\langle R \rangle^2 - \langle R \rangle^2)^{1/2}$ (nm)	$\beta = L/2R$
246.8	42.8	36.3	6.3	3.4

precipitates. The contribution due to DBR is either absent or not significant in the present case. To avoid too much complexity, the extracted single scattering profile was analysed in the light of randomly oriented polydisperse cylindrical particle model with locked aspect ratio. The average length and diameter of the cylinders were estimated to be 246.8 and 72.6 nm., respectively and the aspect ratio was found to be 3.4. The standard deviation of the length distribution and the radius distribution were found to be 42.8 and 6.3 nm, respectively.

References

[1] S Mazumder, D Sen, I S Batra, R Tewari, G K Dey, S Banerjee, A Sequeira, H Amenitsch and S Bernstorff, *Phys. Rev.* **B60**, 822 (1999)
[2] D Sen, S Mazumder, R Tewari, P K De, H Amenitsch and S Bernstorff, *J. Alloys and Compounds* **308**, 250 (2000)
[3] S Mazumder, D Sen, T Saravanan and P R Vijayaraghavan, *J. Neutron Res.* **9**, 39 (2001)
[4] B E Warren, *Acta. Cryst.* **12**, 837 (1959)
[5] S Mazumder and A Sequeira, *Phys. Rev.* **B39**, 6370 (1989)
[6] S Mazumder and A Sequeira, *Phys. Rev.* **B41** 6272 (1990)
[7] S Mazumder, B Jayaswal and A Sequeira, *Physica* **B241**, 1222 (1998)
[8] S Mazumder, D Sen and A K Patra, *J. Appl. Crystallogr.* **36**, 840 (2003)
[9] F B Ramussen, *Colloids and Surfaces* **A187–188**, 327 (2001)
[10] G Beaucage, *J. Appl. Crystallogr.* **28**, 717 (1995)